Mechanical characterization of deep vein thrombosis in a murine model using nanoindentation

K. C. M[c]Gilvray[1], R. Sarkar [2] & C. M. Puttlitz[1]
[1]*Orthopaedic Bioengineering Research Laboratory, Department of Mechanical Engineering and School of Biomedical Engineering, Colorado State University, Fort Collins, CO, USA*
[2]*Northern California Institute for Research and Education, University of California San Francisco, San Francisco, CA, USA*

Abstract

Seventy percent or more of the blood volume is contained by the venous return, and this system of vessels represents a highly distensible, low-pressure configuration. Disease states associated with the venous system have a high impact on society; complications from acute and chronic deep vein thrombosis (DVT), the precursor to post-phlebitic veins (PPV), contribute to more deaths each year than AIDS and breast cancer combined, affecting between 1 and 2% of hospitalized patients in the United States. To our knowledge, there are no published studies with regard to the biomechanical dispensability of either clinical or experimental PPV. To examine the effects of DVT induction on vessel wall biomechanics, a distinct DVT-induced murine model was evaluated. The DVT model was generated using a well-established model via partial ligation of the murine vena cava (MVC). The anisotropic biomechanical properties of each variant were determined along the primary loading axes: circumferential (perpendicular to the surface created by transecting the vein wall longitudinally), longitudinal (perpendicular to the beginning/end surfaces of the isolated intact vessel segment), and luminal (perpendicular to inner surface of vessel) of healthy and diseased vascular tissue via nanoindentation. Three indentation parameters were determined to describe the inherent tissue mechanics: unloading stiffness and two reduced elastic moduli (Oliver-Pharr and JKR formulations). Nanoindentation testing indicated that MVC induced with DVT demonstrated mean deviations (as compared to the normal, baseline tissue) in elastic moduli for the longitudinal and luminal directions. The data also indicate that the unloading stiffness in the longitudinal direction has the largest average magnitude among the three physiologically-relevant planes.
Keywords: nanoindentation, deep vein thrombosis, elastic modulus.

WIT Transactions on Biomedicine and Health, Vol 13, © 2009 WIT Press
www.witpress.com, ISSN 1743-3525 (on-line)
doi:10.2495/BIO090061

1 Introduction

In order to better understand the resultant outcome of deep vein thrombosis (DVT), a technique that has significant spatial resolution must be employed to examine the biomechanical changes of the intra-wall constituents. Therefore, the purpose of this study was to quantitatively compare the structural/material changes through the use of nanoindentation between healthy and DVT-induced veins "diseased", in the three primary axes of loading: in the circumferential (perpendicular to the surface created by transecting the vein wall longitudinally), longitudinal (perpendicular to beginning/end surfaces of the isolated intact vessel segment), and luminal (perpendicular to inner surface of vessel) directions (Figure 1).

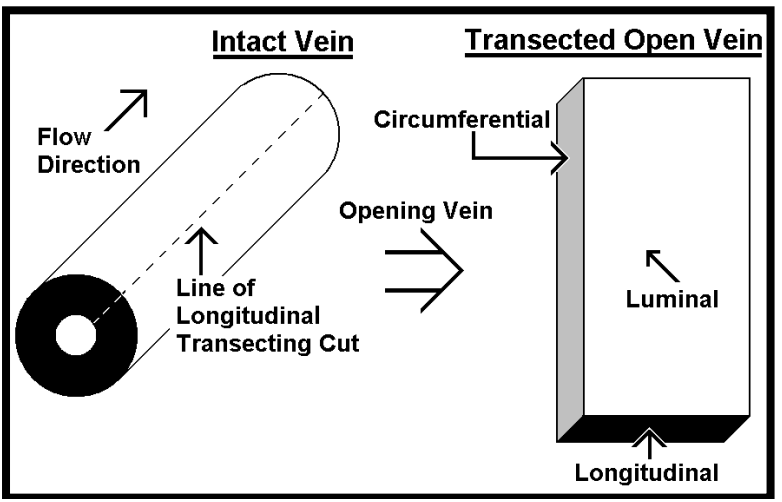

Figure 1: Schematic of IVC sample preparation for nanoindentation testing. The respective biomechanical/physiological loading directions of the vessel wall have been labeled.

Biomechanical properties of vascular tissue on the cellular scale are difficult to evaluate through traditional mechanical testing techniques [4]. Nanoindentation has recently gained popularity for testing soft (elastic modulus ≈ 1MPa) biologic materials on the micrometer length scale [4-7]. This technique utilizes small-diameter spherical tips (approximate 100μm) and micro-scale loads (approximate 100μN) and displacements (1000nm) to obtain accurate measurements in small tissue regions [6]. A number of studies have demonstrated the feasibility of using nanoindentation to elicit biomechanical properties of vascular tissue, yet, to date, few have reported quantitative values comparing healthy and diseased vascular tissue. To our knowledge, no study has examined the biomechanical properties of each of the primary loading axes

(circumferential, longitudinal, and luminal) of healthy and diseased vascular tissue. An understanding of the properties of soft tissues, on all scales, may aid researchers in quantitatively characterizing local mechanics on the cell-to-tissue scale and could clarify relationships between tissue mechanics and pathologic response [8].

Nanoindentation involves application of a controlled load to a surface, with force applications typically ranging between 100nN and 500μN and spatial resolutions between 1nm and 30μm through the use of a nanoindenter [5]. Load-displacement data obtained during one cycle of loading and unloading can be analyzed using equations based on elastic contact theory (Hertzian contact) to quantify structural and material properties such as stiffness and elastic modulus. Currently, the standard technique for analyzing nanoindentation data has been developed and validated for elastic and elastic-plastic materials. The form most often used is that presented by Oliver and Pharr [9] and are based on the classical elastic solutions by Sneddon [10], who derived general relationships between the load, displacement, and contact area for any indenter shape that can be described as a solid revolution of a smooth function [9, 10]. Sneddon demonstrated that the applied load (P) is related to the shear modulus of the material (μ), the radius of contact (a), and the penetration depth (h) through the following relationship:

$$P = \frac{4\mu ah}{1+\upsilon} \quad \text{or} \quad P = \frac{2E\sqrt{A}h}{(1+\nu)^2\sqrt{\pi}} \tag{1}$$

where ν is the Poisson ratio of the material. The elastic modulus (E) of a material is defined as the ratio of normal engineering stress (σ) over engineering strain (ε) in the portion of the stress-strain relationship that obeys Hooke's law.
By taking the first derivative of the applied load with respect to the indenter penetration depth, the unloading stiffness (S) of the substrate can be expressed as a function of the contact area (A) and steady state elastic modulus (E). The compliance of the indenter is considered to be several orders of magnitude less than the compliance of the substrate, and thus can be ignored in the calculation of the elastic modulus. Under these assumptions, the elastic modulus, termed the "reduced modulus" (E_r), can be recast as a function of unloading stiffness and contact area (A_c):

$$E_r = \frac{S\sqrt{\pi}}{2\sqrt{A_c}} \tag{2}$$

The contact area (A_c) between a spherical indenter tip and the substrate can be calculated as follows.

$$A_c = \pi\left(2Rh_c - {h_c}^2\right) \tag{3}$$

where h_c is the contact depth at the maximum load, and R is the nominal radius of the spherical indenter. It has been found empirically that both elastic and plastic deformation may occur during the loading phase, but that the immediate unloading phase is dominated by the elastic response of the substrate material.

That is, even if plastic or viscoelastic deformation occurs in the material, the instantaneous elastic response dominates the initial portion of the unloading curve [5]. Thus, calculating the reduced elastic modulus from nanoindentation data simply involves measuring the unloading stiffness and the contact depth at maximum load (Figure 2).

Since Oliver and Pharr first proposed the formulation for reduced modulus (eqn. (2)) several modification and improvements have been proposed in order to account for deviations from the idealized Hertzian contact conditions. Nanoindentation of soft substrates usually involves a significant adhesive effect between the indenter tip and the sample. The two most common models used to correct for the effects of adhesion on contact mechanics behavior are the Johnson, Kendall, Roberts (JKR) and Deraguin-Muller-Toporov (DMT) models [7]. For low modulus materials, the JKR model, which accounts for adhesion forces only within the expanded area of contact, is considered to give a better representation of the elastic modulus. Specifically, work by Gupta *et al* demonstrated that adhesion plays a significant role in soft tissue contact mechanics [7]. Their investigation concluded that the work of adhesion must be included in the experimental protocol and resulting calculations for determining the mechanical properties with nanoindentation. According to the JKR model, the work of adhesion is related to the magnitude of the maximum tensile pull-off adhesive force, measured during the unloading of the substrate. The authors of this model postulated that the thermodynamic work of adhesion per unit of contact area (W_a) is related to the pull-off adhesion force as follows:

$$F_{pull-off} = \frac{3\pi}{2} R W_a \tag{4}$$

Explicitly, the thermodynamic work of adhesion per unit of contact area (W_a) is the work required to separate two surfaces from finite to infinite contact. This parameter can be directly calculated from the load-displacement profile generated during nanoindentation testing (Figure 2). Using the JKR formulation, the elastic modulus (E_{JKR}) for a spherical indenter can be expressed as:

$$E_{JKR} = \sqrt{\frac{S^3(1-\nu_s{}^2)^2}{6R\left[P+2F_{pull-off}+2F_{pull-off}\sqrt{\left(\frac{P}{F_{pull-off}}+1\right)}\right]}} \tag{5}$$

where S is the unloading stiffness, R is the nominal radius of the indenter tip, and $F_{Pull\text{-}off}$ is a measure of the adhesion force generated during tip-substrate separation. The JKR model (eqn. (5)), which accounts for interfacial forces outside the Hertzian contact area, is the most applicable adhesion model for compliant materials indented with spherical probes with a large radius of curvature (approximate 100μm) [7].

2 Materials and methods

Nanoindentation tests were performed on both healthy and DVT induced ("diseased") murine inferior vena cava tissue (IVC) (n = 8 IVC/group) [3].

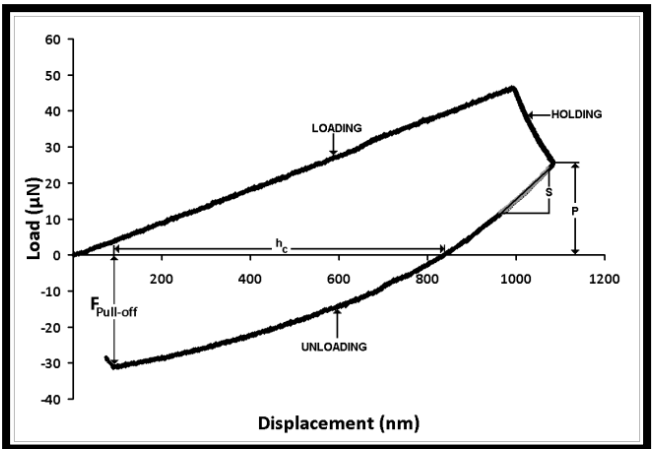

Figure 2: Typical load-displacement curve observed during nanoindentation testing of murine vena cava. Biomechanical indices used in the formulation of equations (2) and (5) are indicated.

Diseased murine vena cava tissue samples were created by causing a partial stenosis for seven days via tightening a suture around the IVC of a mouse until blood flow was reduced by 80-90%, invariably producing occlusive, laminar thrombi [3, 11]. Harvested IVC were transected longitudinally along the flow direction, creating a planar sheet. The thrombus was then separated from the vessel wall for the diseased group. Each planar murine sample was sectioned circumferentially into three equal samples sections. Samples were stored in cool (approximately 20ºC) isotonic saline (0.9%w/v sodium chloride) and biomechanically tested within forty-eight hours post sacrifice. Care was taken to ensure that the primary directions of physiological loading (circumferential, longitudinal, and luminal) were "tracked" through all processing procedures for each piece of tissue. Prior to nanoindentation testing, the samples were mounted using previously reported techniques [4-6], which have been shown to maintain sample hydration for up to eight hours and provide adequate mechanical substrate support for testing [4]. To insure complete equilibrium hydration testing, samples were submerged in saline at forty-five minute intervals for a minimum of twenty minutes. Using these dissection and hydration techniques, it was possible to mount hydrated samples such that one of the six sides from each planar sheet was aligned in one of the primary directions of interest.

Nanoindentation measurements were performed using a Hysitron TriboIndenter (Hysitron Inc., Minneapolis, MN). A 100μm, 90º cone angle fluid cell nonporous diamond tip was used for all experiments. Ebenstein *et al* showed a conospherical diamond probe, with a 100μm radius of curvature was found to be suitable for testing a variety of soft hydrated materials [4]. Their work demonstrated repeatable measurement on all of the materials they tested, exhibited minimal approach problems, and had reasonable projected contact area

to measure local tissue properties rather than individual cells or globally averaged tissue properties [4]. A trapezoidal loading profile was selected; once the tip was brought into contact with the sample, the load was applied at a rate of 100 μN/s, held for 10 seconds at the maximum load (400 μN) to permit viscoelastic dissipation, and subsequently withdrawn at a rate of 100 μN/s [4, 6, 7]. For these experiments much of the applied load was associated with moving the tip at large displacements, the actual peak load imparted on the samples ranged from 10–80 μ*N* (Figure 2). A trapezoidal load function was utilized to allow creep in the substrate to dissipate prior to unloading. Load–displacement curves were corrected for large displacements and 8 μ*N* force offsets were imposed prior to the analysis. Brisceo et al. demonstrated that this loading profile, while not long enough for creep to fully dissipate, was sufficient for the unloading behavior to dominant the inherent viscoelastic effects [12]. Load and displacement were recorded simultaneously during indentation at 228 Hz. Three parameters are reported here as measures of tissue mechanical properties: the unloading stiffness, reduced elastic modulus [9] (Oliver-Pharr formulation, eqn. (2)), and JKR elastic modulus (eqn. (5)) [13]. Because an identical load function was applied to each indenter site, the changes in the indentation response of the tissue, as quantified by these parameters, provide a measure of relative functional properties in the different tissue specimens [4]. The unloading stiffness, (*S*), was calculated by fitting a linear function to the initial 10% portion of the unloading curve.

Statistical significance in the aforementioned biomechanical parameters between groups was performed using a student's t-test (SigmaStat, Systat Software Inc. Richmond, California, USA), p-values less than 0.05 were considered statistically significant.

3 Results

Using the JKR formulation of elastic modulus, which is considered to be the most accurate for "soft" biomaterials, the data indicate that the mean elastic moduli of healthy murine IVC ranges from 238.1 kPa in the luminal direction to 362.6 kPa in the circumferential direction. The mean elastic modulus in the longitudinal direction was 270.5 kPa. The DVT-induced samples had mean elastic moduli of 340.5 kPa in the luminal direction, 397.3 kPa in the circumferential direction, and 381.1 kPa in the longitudinal direction.

No statistically significant differences between the healthy and diseased tissue was found for the unloading stiffness parameters in the three orthogonal directions. However, statistical differences were observed intra-group (Table 1). The longitudinal unloading stiffness of the healthy tissue demonstrated a statistical increase of 43.6% and 62.5% as compared to the circumferential and luminal directions, respectively (Figure 3). Similarly the diseased tissue showed a statistically significant increase in the unloading stiffness in the longitudinal direction of 40.5% and 62.2% when compared to the circumferential and luminal direction, respectively (Figure 3).

Table 1: Unloading stiffness formulations in the circumferential, longitudinal, and luminal directions based on nanoindentation data for healthy and diseased (induced with deep vein thrombosis) groups. Calculated means are shown with (±) one standard deviation. Similar letters correspond to the given p-values.

Unloading Stiffness (μN/nm)			
	Circumferential	Longitudinal	Luminal
Healthy	0.0275 ± 0.0120^{A} (A) p = 0.340	0.0440 ± 0.0127^{B} (B) p = 0.117	0.0192 ± 0.0080^{C} (C) p = 0.736
Diseased	0.0319 ± 0.0024^{A}	0.0513 ± 0.0099^{B}	0.0208 ± 0.0049^{C}
In Heathly:		*In Diseased:*	
Radial > Longitudinal	p = 0.002	Radial > Longitudinal	p < 0.001
Luminal > Longitudinal	p < 0.001	Luminal > Longitudinal	p < 0.001

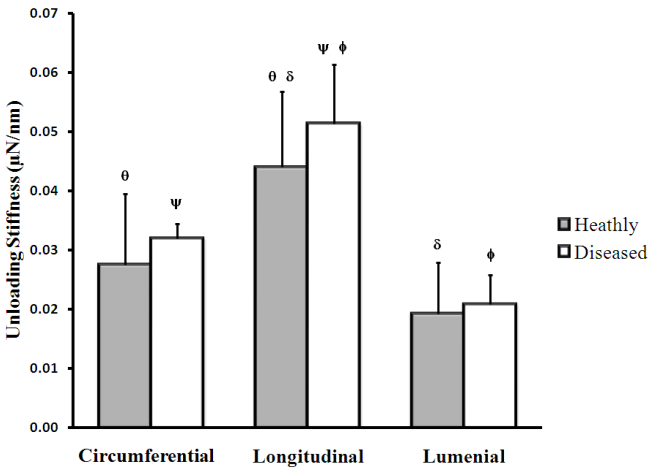

Figure 3: Unloading stiffness calculated from nanoindentation data in the three primary axes of loading. Averages are shown with one standard deviation error bars, with similar letters indicating statistical differences. Statistically significant p-values are as follows: (θ) p =0.002, (ψ) p < 0.001, (δ) p < 0.001, (φ) p < 0.001.

All reduced elastic moduli calculations were statistically different ($p<0.05$) from the corresponding JKR elastic moduli calculations, for the three primary directions of interest. No statistically significant findings were noted between the healthy and diseased tissue in the circumferential direction (Table 2). The circumferential direction did demonstrate a non-significant increase of 9.51% between the healthy and diseased tissue for the JKR elastic modulus formulation. The longitudinal reduced elastic modulus was statically greater (111.8%) for the diseased tissue as compared to the healthy tissue (Table 2, Figure 4). The longitudinal JKR elastic modulus for the diseased tissue was not statistically different than that of the healthy tissue; however, an increase of 40.9% was calculated for the diseased tissue. The luminal JKR elastic modulus was statistically greater (43%) for the diseased tissue compared to the healthy tissue, (Table 2, Figure 5).

Table 2: Elastic modulus formulations (reduced and JKR) in the circumferential, longitudinal, and luminal directions based on nanoindentation data for healthy and diseased (induced with deep vein thrombosis) groups. Calculated means are shown with (±) one standard deviation. Similar letters correspond to the given p-values.

CIRCUMFERENTIAL PARAMATERS

	Reduced Elastic Modulus (MPa)		Elastic Modulus JKR (MPa)	
Healthy	0.6108 ± 0.1819 [A]	(A) p = 0.583	0.3626 ± 0.1207 [B]	(B) p = 0.579
Diseased	0.6455 ± 0.1132 [A]		0.3973 ± 0.0424 [B]	

LONGITUDINAL PARAMATERS

	Reduced Elastic Modulus (MPa)		Elastic Modulus JKR (MPa)	
Healthy	0.4558 ± 0.0222 [C]	(C) p < 0.001	0.2705 ± 0.0153 [D]	(D) p = 0.201
Diseased	0.9654 ± 0.3243 [C]		0.3811 ± 0.0902 [D]	

LUMINAL PARAMATERS

	Reduced Elastic Modulus (MPa)		Elastic Modulus JKR (MPa)	
Healthy	0.4651 ± 0.1007 [E]	(E) p = 0.086	0.2381 ± 0.0461 [F]	(F) p = 0.024
Diseased	0.5412 ± 0.0985 [E]		0.3406 ± 0.0854 [F]	

NOTE: ALL Reduced Elastic Modulus calculations where statically different from the corresponding JKR Elastic Modulus calculations $p < 0.05$.

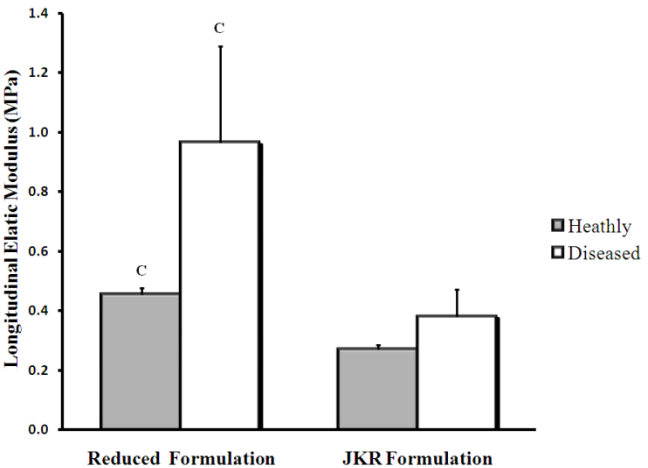

Figure 4: Elastic moduli (reduced and JKR formulations) calculated from nanoindentation data in the longitudinal axes of loading. Averages are shown with one standard deviation error bar, with similar letters indicating statistical differences. Statistically significant p-values are as follows: (C) $p < 0.001$.

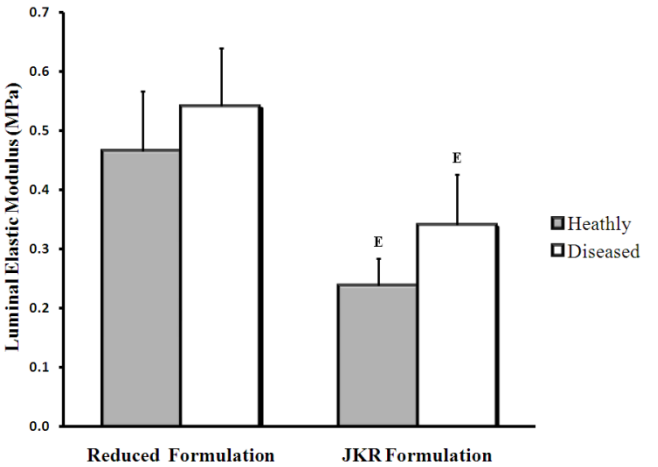

Figure 5: Elastic moduli (reduced and JKR formulations) calculated from nanoindentation data in the luminal axis of loading. Averages are shown with one standard deviation error bar, with similar letters indicating statistical differences. Statistically significant p-values are as follows: (E) $p = 0.024$.

4 Discussion

Nanoindentation is a compressive testing process. This type of testing does not explicitly mimic the physiologic *in vivo* loads expected. However, nanoindentation does give insight into general comparisons of the biomechanical response of the tissue. The assumption used for this analysis is that relationships between the compressive load histories can be applied to the more physiologically-relevant tensile loading history. This is to say that the compressive-tensile anisotropy is known to exist *in vivo*, however in order to make conclusions based on the presented nanoindentation data the underlying assumption is that the *in vivo* tensile response of the tissue is altered in a manner that is similar to our indentation data.

The results presented above further emphasis that the formulation used to calculate the elastic modulus of the material based on nanoindentation data is crucial in determining accurate biomechanical response parameters. This is apparent when considering that all of the reduced elastic moduli calculations were statistically different from the corresponding JKR formulation of the elastic moduli.

Interestingly, the longitudinal unloading stiffness was statistically greater than the circumferential or luminal responses. This could possibly be correlated to the physiologic *in vivo* response of the tissue, were the tissue is generally under circumferential stress rather than longitudinal or luminal stresses. It is hypothesized by our group that increased stiffness in the longitudinal direction in a 3D loading case is important in maintaining physiologic hemostasis and can be

directly correlated to collagen and elastin fiber alignment within the tissue. Future finite element and histological work by our lab will address this hypothesis.

The only statistical difference from normal, healthy baseline data based on the JKR elastic modulus formulation was noted in the luminal direction. This correlates with previously published data examining only the luminal surface of vascular tissue [4, 5]. Surprisingly, no statistical changes where observed in the circumferential and longitudinal direction. Clinically, increases in intra-luminal pressure following DVT are associated with a reduced capability of the vessel to distend [14]. The DVT model used here has previously demonstrated strong histologic correlation to clinically recovered DVT veins [3]. The data presented within seems to indicate that even non-statistical changes in the circumferential and longitudinal response parameter coupled with statistical changes only in the luminal direction can have a large affect on the response of the tissue (and the entire venous system). In order to address these issues a more comprehensive battery of biomechanical tests are currently being performed by our lab, including bi-axial stretch experiments, strain energy function fitting, and finite element modeling.

References

[1] Azuma T, Hasegawa M. Distensibility of the vein: from the architectural point of view. Biorheology 1973; 10: 469-79.
[2] Anderson FA, Jr., Wheeler HB. Physician practices in the management of venous thromboembolism: a community-wide survey. J Vasc Surg 1992; 16: 707-14.
[3] Humphries J, McGuinness CL, Smith A, Waltham M, Poston R, KG B. Monocyte chemotactic protein-1 (MCP-1) accelerates the organization and resolution of venous thrombi. J Vasc Surg 1999; 30: 894-9.
[4] Ebenstein L, Pruitt L. Nanoindentation of soft hydrated materials for application to vascular tissues. J Biomed Mater Res A. 2004; 69: 222-232.
[5] Ebenstein D. Biomechanical Characterization of Atherosclerotic Plaques: A Combined Nanoindentation and FTIR Approach. In Bioengineering: Dissertation, University of California, Berkeley; 2002.
[6] Ebenstein D, Kuo A, Rodrigo J, Reddi A, Ries M, Pruitt L. A nanoindentation technique for functional evaluation of cartilage repair tissue. J. Mater. Res. 2003; 19: 273-281.
[7] Gupta S, Fernando C, Cheng L, Pruitt L, Puttlitz C. Adhesive forces significantly affect elastic modulus determination of soft polymeric materials in nanoindentation. Materials Letters 2007; 61: 448-451.
[8] Jacot J, Dianis S, Schnall J, Wong J. A simple microindentation technique for mapping the microscale compliance of soft hydrated materials and tissues. Journal of Biomedical Materials Research 2006: 485-494.
[9] Oliver WC, Pharr GM. An Improved Technique for Determining Hardness and Elastic Modus Using Load and Displacement Sensing Indentation Experiments. Journal of Material Research 1992; 7: 1564-1584.

[10] Sneddon IN. The relation between load and penetration in the axisymmetric boussinesq problem for a punch of arbitrary profile. Int J Engng Sci 1965; 3: 47-57.
[11] McGuinness CL, Humphries J, Smith A, Burnand KG. A new model of venous thrombosis. Cardiovasc Surg 1997; 5.
[12] Briscoe B, Fiori L, Pelillo E. Nano-indentation of polymeric surfaces. Journal of Physics D-Applied Physics 1998; 31: 2395-2405.
[13] K.L. Johnson K. Kendall, A.D. Roberts. Surface energy and the contact of elastic solids. Proc R. Soc. Lond. 1971; A324: 310-313.
[14] Dobrin PB. Mechanics of normal and diseased blood vessels. Ann Vasc Surg 1988; 2: 283-94.